

DYNAMICS OF CLOGGING PROCESSES IN INJECTION WELLS USED TO PUMP HIGHLY MINERALIZED THERMAL WATERS INTO THE SANDSTONE STRUCTURES LYING UNDER THE POLISH LOWLANDS

BARBARA TOMASZEWSKA*, LESZEK PAJĄK**

Mineral and Energy Economy Research Institute – Polish Academy of Sciences
Department of Renewable Energy and Environmental Research
Division of Renewable Energy

Corresponding author's e-mails: *tomaszewska@meeri.pl, **pajak@meeri.pl

Keywords: Geothermal waters, injection well, sedimentation, mineral deposition.

Abstract: When identifying the conditions required for the sustainable and long-term exploitation of geothermal resources it is very important to assess the dynamics of processes linked to the formation, migration and deposition of particles in geothermal systems. Such particles often cause clogging and damage to the boreholes and source reservoirs. Solid particles: products of corrosion processes, secondary precipitation from geothermal water or particles from the rock formations holding the source reservoir, may settle in the surface installations and lead to clogging of the injection wells. The paper proposes a mathematical model for changes in the absorbance index and the water injection pressure required over time. This was determined from the operating conditions for a model system consisting of a doublet of geothermal wells (extraction and injection well) and using the water occurring in Liassic sandstone structures in the Polish Lowland. Calculations were based on real data and conditions found in the Skiermiewice GT-2 source reservoir intake. The main product of secondary mineral precipitation is calcium carbonate in the form of aragonite and calcite. It has been demonstrated that clogging of the active zone causes a particularly high surge in injection pressure during the first 24 hours of pumping. In subsequent hours, pressure increases are close to linear and gradually grow to a level of ~2.2 MPa after 120 hours. The absorbance index decreases at a particularly fast rate during the first six hours (Figure 4). Over the period of time analysed, its value decreases from over 42 to approximately 18 m³/h/MPa after 120 hours from initiation of the injection. These estimated results have been confirmed in practice by real-life investigation of an injection well. The absorbance index recorded during the hydrodynamic tests decreased to approximately 20 m³/h/MPa after 120 hours.

INTRODUCTION

In addition to corrosion, the precipitation and sedimentation of mineral compounds (scaling) is one of the key problems associated with the exploitation of geothermal water. These processes often lead to the clogging of the inside of installation components and source reservoir rock formations, thus limiting their exploitation capacity, in particular the re-injection of water, by reducing productivity and absorbance capacity. This has an impact on the costs of equipment and the exploitation of geothermal facilities and therefore on the costs of obtaining energy from the system. In extreme situation this may cause the need to

temporarily shut-down the installation or some of its components. This phenomenon occurs at varying degrees of severity in several geothermal installations in Poland and abroad.

The injection of used geothermal liquids (cooled through the recovery of energy in surface installations) requires the overcoming of resistance consisting of load loss in boreholes, pressure loss related to the injection of liquid into the water carrying layer and the skin effect (losses of load caused by the layer directly adjacent to the filter). Polarisation of concentrations and changes in the thermodynamic status of water often lead to the precipitation of secondary sediments on top of the above. The intensity of scaling mainly depends on physical properties and chemical composition of water, more particularly on carbonate hardness, flow velocity, temperature and pressure [2, 16, 18]. Secondary mineral deposition often results in scaling of the active sections of the filter and gravel filtration pack in injection wells and change in the primary properties of the source reservoir rock formations such as density, porosity and permeability [3].

Assessment of the propensity of sediment precipitation and clogging of the active zone in injection wells is one of the key elements of the studies to be considered, and already taken into account, at the design stage of geothermal installations, the opening and testing water resources and also at the stages of exploitation and re-injection of the water [5, 7, 8, 9, 11, 12, 16, 17, 18]. This issue plays a particularly important role in the re-injection of highly mineralized brine into porous sandstone formations. The paper proposes a mathematical model for describing how the absorption index and water injection pressure required changes with time under operating conditions modeled on a well doublet (exploitation-injection borehole) for water resources in the Liassic sandstone structures of the Polish Lowlands. The calculations were based on real data from the Skierniewice GT-2 well intake area.

PARAMETERS OF THE RESOURCE RESERVOIR ROCK FORMATION AND CONSTRUCTION OF THE INJECTION WELL ZONE

The key rock formations at the study site are the Kłodawa strata (lower Liassic – hetang, synemur) of the lower Jurassic series which are formed of sandstones intersected with interrupted series of low-permeability or impermeable sediments (compact fine-grain sandstone, mudstones and claystones). The most important impermeable complex is the lower toarsian clay- and mudstone formation.

Theoretical analyses were carried out based on data derived from the exploitation of the Skierniewice GT-2 well. The active zone of the injection borehole stretches across the upper Kłodawa strata, which can be exploited between the depths of 2771 m and 2886 m (see Figure 1a).

A multi-section Johnson's screen has been installed in the borehole with its active sections in the following intervals: 2801.66–2825.73, 2843.78–2849.80, 2855–2893.84 m (a total length of 48.13 m) (Figure 1b). The filter gap is 0.5 mm, and the total surface of the gaps accounts for 10% of the overall filter surface. Before installation of the filter, the borehole was expanded up to a diameter of 432 mm (450 mm in some sections) in the 2801–2886 m. The filter section is filled with gravel pack of a grain size ranging from 1.0 to 2.2 mm [1]. The upper section of the filter interval is lithologically diverse, with packs of compact, fine-grain sandstone with layers of mudstone and claystone, there are also some secondary low-uniformity sandstone formations. The effective porosity is

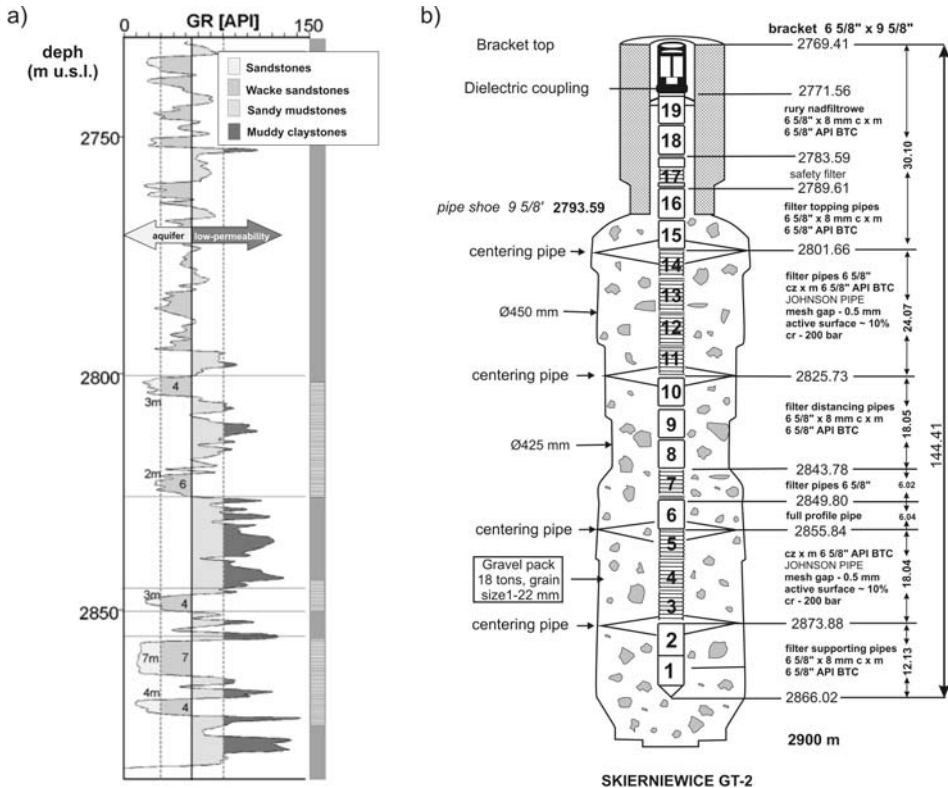


Fig. 1. Active zone in an injection well: a) share of sandstone formation in the lithological profile of the Upper Klodawa strata open to exploitation (based on [19]), b) construction diagram of the Johnson's filter in the injection well (based on [1])

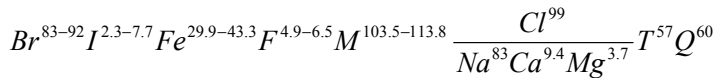
7–14% and the permeability is 1–180 mD. Lithological diversity is also significant in the lower sections of the borehole, with packs of loose, coarse grain sandstone with the best collector properties, but their thickness is low (3 to 7 m). There are micro-gaps present in that section. Porosity ranges from 11% to 18% and the permeability varies between 38 and 6800 mD, with the high values (1200–6800 mD) identified in the coarse and medium grained sandstones, and sometimes also in other friable formations [1].

The analysis of the GR profiling showed that the active section of the filter in the injection well investigated opens only 19 m of the sandstone layer, while the rest of the profile consists mainly of mudstone and claystone [4].

PHYSICAL PROPERTIES AND CHEMICAL COMPOSITION OF THE THERMAL WATER

Mineralisation of the geothermal water pumped from the exploitation well ranges from 101.5 g/dm³ to 113.8 g/dm³. The water is slightly acidic (pH around 6.45 – field measurement). It represents a reductive environment (Eh = -515--200 mV). The temperature of the water at the pumping speed of 60 m³/h is 57.2°C. The ion pool is

dominated by chloride anions Cl^- – 99.3% mval, and sodium cations Na^+ – 86.3% mval. According to the Altowski-Szwiec classification system, the water is of a Na–Cl chemical type. Carbonate hardness varies within the range of 139.4 to 214.5 $\text{mgCaCO}_3/\text{dm}^3$ and the general hardness ranges from 11000.5 to 12431 $\text{mgCaCO}_3/\text{dm}^3$. Concentration of Ca^{2+} calcium is 3184 to 3826 mg/dm^3 corresponding to 9.4% mval, magnesium Mg^{2+} , cations range from 700.7 to 778.8 mg/dm^3 and sulphate anions SO_4^{2-} from 328.6 to 580.7 mg/dm^3 . The chemical composition of the water shows an increased content of micro-elements: iron (29.89–49.29 mg/dm^3), strontium (105.4–150.5 mg/dm^3), bromides (83–92 mg/dm^3), iodine (2.3–7.7 mg/dm^3) and fluorides (4.93–6.46 mg/dm^3). The chemical formula of the water according to Kurlov is described as follows:



METHODOLOGY OF THE ANALYSES

To estimate the clogging dynamics of the injection well, geochemical modeling was first performed (using the PHREEQCI software, version 2.17, [14]) and this has been further used to determine the quantitative and qualitative tendency for precipitation of secondary sediments from the thermal water. This information was then used to evaluate the decrease in absorbance and to forecast changes in pressure necessary to inject the cooled waters into the rock formation. The mathematical modeling of the effects related to clogging of the active zone was based on calculation algorithms taking into account:

- Flow resistance in the borehole, described with the following equation [15]:

$$\Delta p_p = \lambda \frac{L}{d} \frac{\rho}{2} w^2 \quad (1)$$

where:

Δp_p – flow resistance related to the flowing of liquid through the geothermal borehole [Pa],

λ – friction coefficient (dimensionless) [-],

L – length of the geothermal borehole [m],

d – internal diameter of the geothermal borehole [m],

ρ – density of the geothermal liquid [kg/m^3],

w – liquid flow velocity in the borehole [m/s].

- Resistance resulting from injecting the liquid into the source formation, described by the equation [10]:

$$\Delta p_w = \frac{V \mu}{4 \Pi k_h h} \ln \left(\frac{2.25 k_h \tau}{\phi \mu c_t r_w^2} \right) \quad (2)$$

where:

τ – time, after which the value of repression stabilizes (Δp_w) [s],

ϕ – effective porosity of the water bearing stratum skeleton (ratio of the volume open to flow and total volume, dimensionless parameter) [-],

c_t – medium compression coefficient [1/Pa].

Relationship (2) is true assuming that: the thickness of the layer is constant and infinite, flow within the layer is laminar and horizontal only, the layer is completely crossed by the filter, permeability of the layer is isotropic, the viscosity of the liquid does not vary within the layer (it is not, for instance, a function of pressure and temperature), the layer is completely saturated with the liquid, the stream of injected liquid is invariable in time and that there are no interactions between the injection and exploitation wells.

- Resistance generated by the water bearing layer in the filter zone (the so-called skin effect), according to [10]:

$$s = \left(\frac{k}{k_s} - 1 \right) \ln \left(\frac{r_{wa}}{r_w} \right) + \left(\frac{h}{h_p} - 1 \right) \left(\ln \left(\frac{h}{r_w} \sqrt{\frac{k_h}{k_v}} \right) - 2 \right) + \left(\frac{\mu_{t1} \rho_{t0}}{\mu_{t0} \rho_{t1}} \ln \left(\frac{r_s}{r_w} \right) + \ln \left(\frac{r_d}{r_s} \right) \right) \quad (3)$$

where:

- s – dimensionless skin effect coefficient [-],
- k – natural permeability of the water bearing layer [m²],
- k_s – permeability of the borehole zone [m²],
- r_{wa} – range – radius of the damaged/affected zone [m],
- h_p – thickness of the layer covered by the filter [m],
- k_v – vertical permeability of the water bearing layer [m²],
- μ_{t1} – dynamic viscosity of the liquid injected, at injection temperature [Pa s],
- μ_{t0} – dynamic viscosity of the liquid injected at the natural source layer temperature [Pa s],
- ρ_{t1} – density of the liquid injected at injection temperature [kg/m³],
- ρ_{t0} – density of the liquid injected at the natural source layer temperature [kg/m³],
- r_s – radius of the cool front (calculated assuming a “piston-effect” displacement of water from the source layer by the injected water) [m].
- r_d – radius of change in pressure, caused by injection [m].
- Impact of the change in properties of the liquids injected on the repression pressure (viscosity μ_0 and density ρ_0), determined using the following formula [13]:

$$\rho_0 = 16,018 \cdot (62.368 + 0.438603 S + 1.60074 \cdot 10^{-3} S^2) \quad (4)$$

where:

- ρ_0 – density of the brine under standard conditions [kg/m³],
 - S – salinity (mass fraction of substances dissolved in the brine) [%].
- and

$$\mu_0 = A (T')^{-B} \cdot 10^{-3} \quad (5)$$

$$A = 109.574 - 8.40564 S + 0.313314 S^2 + 8.72213 \cdot 10^{-3} S^3$$

$$B = 1.12166 - 2.63951 \cdot 10^{-2} S + 6.79461 \cdot 10^{-4} S^2 + 5.47119 \cdot 10^{-5} S^3 - 1.55586 \cdot 10^{-6} S^4$$

where:

- μ_0 – dynamic viscosity of the brine under pressure at source formation temperature

- Impact of the heat exchange between the brine and the geological environment, based on the following formula [6]:

$$q_{\text{str}} = \frac{-4\pi \lambda_g (t_s - t_\infty)}{\ln\left(\frac{4 a_g \tau}{r_w^2} - 2\gamma\right)} \quad (6)$$

where:

- q_{str} – unit power losses occurring in the heat exchange between the liquid and the geological environment, per metre of borehole length [W/m],
- λ_g – heat transfer coefficient of the geological environment [W/(m K)],
- t_s – temperature of the brine [°C],
- t_∞ – natural temperature of the geological environment, before injection or at significant distance from the borehole (outside the range of thermal impact) [°C],
- a_g – temperature equalization coefficient of the geological environment [m²/s],
- τ – time, after which the heat exchange stabilizes [s],
- γ – Euler's constant ($\gamma=0.577216\dots$) [-].

The required injection pressure is determined by the following formula:

$$\Delta p = \Delta p_p + \Delta p_w + \Delta p_s - H_z \rho_{\text{sr}} g - (H_w - H_z)(\rho_{\text{sr}z} - \rho_{\text{sr}n})g \quad (7)$$

where:

- Δp – total required excess pressure to be generated by the injection pumps [Pa],
- H_z – level of the static water table, calculated versus ground surface [m],
- H_w – depth of the borehole [m],
- ρ_{sr} – averaged density of the liquid injected in the borehole, above the static water table [kg/m³],
- $\rho_{\text{sr}z}$ – average density of the liquid injected into the source formation layer at the depth interval of H_z to H_w [kg/m³],
- $\rho_{\text{sr}n}$ – average density of the liquid in the borehole, under natural conditions, at the depth interval from H_z to H_w [kg/m³],
- g – earth gravity [m/s²].

The absorbance index q_c , [m³/s / Pa], expressing the ratio between the stream of liquid being injected into the source layer and the excess pressure to be generated by the injection pumps has been defined as follows:

$$q_c = \frac{V}{\Delta p} \quad (8)$$

where:

- V – stream of injected water [m³/s],
- Δp – pressure head generated by the injection pumps [Pa].

Precipitation of secondary sediments from the thermal water

Figure 2 shows thermodynamic equilibrium distributions of the water analysed within the temperature range of 20°C to 80°C. These indicate that water at a source layer temperature of 68°C is saturated mainly with the rock minerals from the reservoir, i. e., silicates, aluminosilicates as well as clay and carbonate particulates. The analyses also demonstrated super-saturation of the water with iron-based minerals: goethite and hematite. Sulphate-based minerals (anhydrite and gypsum) can dissolve in water.

The water is super-saturated with carbonate mineral phases at a temperature of 50°C (temperature of the water injected in the rock formations during the absorbance tests).

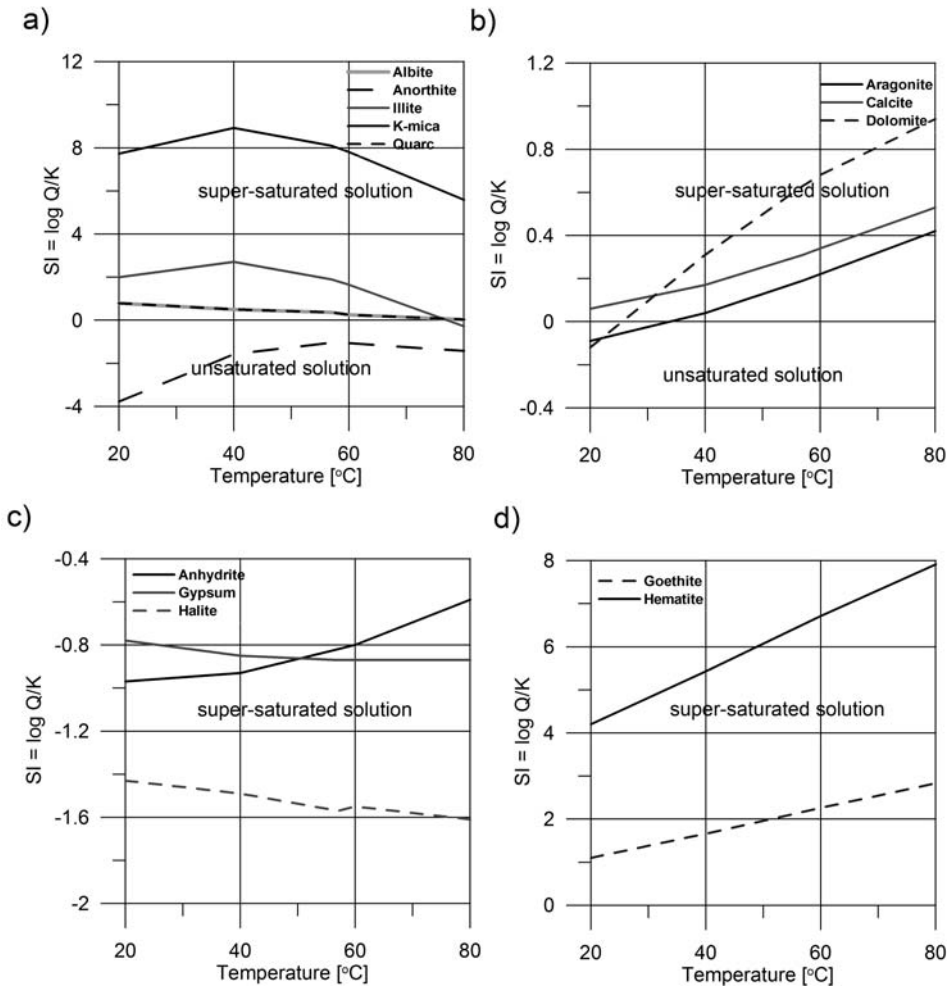


Fig. 2. Changes in the Saturation Index (SI) versus selected mineral phases as a function of temperature of the geothermal water injected into the rock formation: a) silicates, aluminosilicates and clay minerals, b) carbonates, c) sulphates and halites, d) iron-based minerals

At a temperature of 50°C (temperature of the water injected into the rock formation when carrying out the absorbance tests), water is super-saturated with carbonate mineral phases (aragonite, calcite and dolomite), silicate phases, aluminosilicates and clay minerals: albite, illite, K-mica, kaolinite, quartz and iron-based forms, mainly oxides and oxyhydroxydes (goethite and hematite) (Figure 2). Taking into account the thermodynamic parameters of the water under the conditions described, it has been estimated that the amount of sedimentation in the immersed filter zone can reach 0.063 mg/dm³ of solids, mainly in the form of aragonite. At a flow intensity of 25 m³/h this corresponds to approximately 1.5 kg of calcium carbonate, and at 50 m³/h, twice that amount, i.e. approximately 3 kg per hour (the length of the active section of the filter is 48.13 m).

Dynamics of the clogging process in the active area

The dynamics of the clogging process in the injection well and the resulting changes in the absorbance index and the pressure required to inject cooled water into the source rock formation were analysed based on the following assumptions:

- Construction of the injection borehole:

Depth interval [m]	Borehole diameter (d_w), [cal]
0 – 278	13 7/8
278 – 2769.4	9 5/8
2769.4 – 2886	6 5/8

- A stream of highly saline brine injected into the rock formation at: 40 m³/h,
- Temperature of the injected brine: 50°C at the head of the injection borehole,
- 11% salinity,
- Heat transfer coefficient of the geological environment (λ_g): 2.5 W/(m K), density of the rock formation environment 2.4 Mg/m³, specific heat of the rock formation 0.8 kJ/(kg K),
- Change in temperature in the borehole area in line with the geothermal gradient, from the source layer temperature of 70°C to the surface temperature of 8°C,
- Effective porosity of the water bearing stratum 15%,
- Thickness of the water bearing horizon 64 m, thickness covered by the borehole and thickness of the permeable layer: 19 m,
- Permeability of the water bearing stratum: horizontal – 210 mD and vertical – 21 mD,
- Level of the static water table 125 m u.l.s.l. (under land surface level),
- Range of the zone affected by the skin effect – 1.25 m and its permeability – 10 D (the commissioning documentation suggested a negative value of the hydraulic skin effect coefficient leading to such a high value of permeability),
- The forecast time of water injection is counted from the start-up of the borehole after cleaning the scale products causing the clogging (after acid treatment),
- The quantity of products causing the clogging in the filter zone is 0.063 kg/m³. It has been determined based on analyses that take the chemical composition of water into account,

It has been assumed that the products of secondary clogging sediment in the internal parts of the filter and gravel pack and have a permeability of 7 mD.

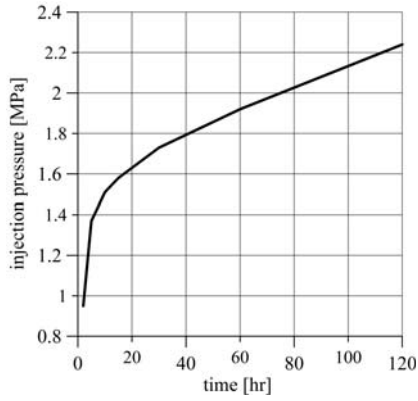


Fig. 3. Forecast changes in the injection pressure required with time, assuming a 40 m³/h constant flow of brine injection

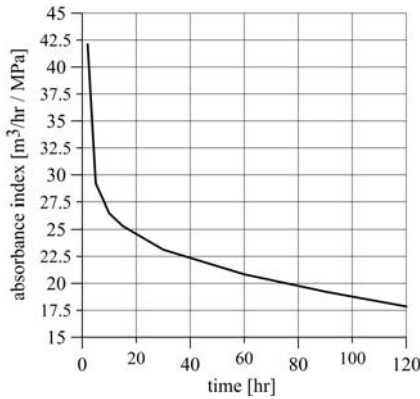


Fig. 4. Forecast changes in the absorbance index with time, assuming a 40 m³/h flow of brine injection

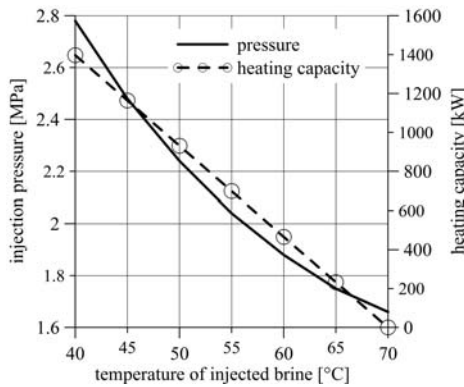


Fig. 5. Forecast changes in injection pressure and thermal capacity of the doublet 120 hours from start-up of a cleaned injection well, at a constant flow of exploited and injected water (40 m³/h)

The results of calculations based on the model are shown in Figures 3 to 6. A gradual change in injection pressure is shown in Fig. 3 which results from clogging in the active zone.

The forecast shows the injection pressure increasing particularly rapidly in the first 24 hours of pumping. In the subsequent hours of the analysed period the increase in pressure is close to linear and continual, reaching a value of ~ 2.2 MPa at 120 hours. The value of the absorbance index declines, more particularly in the first six hours (Fig. 4). In the investigated period, the value decreases from more than 42 C to approximately $18 \text{ m}^3/\text{h}/\text{MPa}$ at 120 hours after initiation of the injection. The results of analyses based on the model were verified with absorbance tests in the injection borehole, using the same flow intensity and temperature of the water injected into the source rock formation. The results of the forecasts and real measurements taken at the borehole are comparable. The absorbance index measured during hydrodynamic tests dropped down to approximately $20 \text{ m}^3/\text{h} / \text{MPa}$ after 120 hours.

Figure 6 shows the variability of the absorbance index and injection pressure over 120 hours as a function of stream of brine exploited by the geothermal doublet. In the hydro-geothermal conditions analyzed, a sudden drop in absorbance index is being observed when the injection capacity is $50 \text{ m}^3/\text{h}$. Above the value of $50 \text{ m}^3/\text{h}$, the value of the absorbance index decreases at a much slower pace.

The key product of secondary mineral precipitation from the geothermal water in the system investigated is calcium carbonate in the form of aragonite and calcite. The geo-chemical modeling performed has demonstrated a tendency to precipitate these crystalline forms of CaCO_3 . Calcite is the more stable phase, usually forming through re-crystallization of aragonite, which is the less stable form of calcium carbonate – the first one to form in the process of mineral precipitation from the solution, more particularly from higher temperature waters (including geothermal water). The presence of these minerals has been demonstrated in samples of materials discharged from the borehole during implementation of the source zone cleaning procedures. Secondary precipitation products and products of corrosion of the pipes coat the filter and the gravel pack, and are carried with the injected water so penetrating the reservoir rock

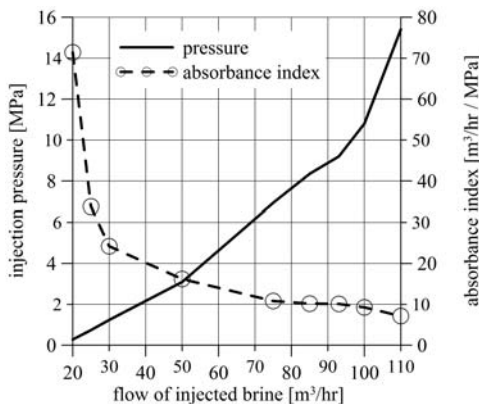


Fig. 6. Forecasted variation of the absorbance index and injection pressure with flow of the injected liquid, 120 hours from initiation of injection into the source rock formation

formations (probably they are also deposited and form accumulation clusters in the structures of the reservoir rock). As a result, absorbance of the boreholes, borehole zone and source rock formations is decreasing and this has been clearly demonstrated in the analyses performed based on the model and in the practical results from the injection of water into the rock formations.

The above-mentioned processes and observed consequences may have various levels of intensity, depending on the flow and temperature of water streams injected into the rock formation. Figure 6 shows the relationship between the absorbance index and the flow of injected brine, suggesting a dramatic and sudden drop of the index in the flow range up to 50 m³/h. After exceeding 50 m³/h, the value of the absorbance index decreases at a slower rate – of course an increase in the injection pressure required is still observed.

SUMMARY

Analysing the impacts of particular factors on conditions linked to the re-injection of mineralized waters into the source rock formation, one can conclude that due to the number of variables involved, the mathematical description of the process is both complicated and ambiguous. The mathematical description of the physical properties of mineralized brines, as a function of their pressure, temperature, physical properties and chemical composition, requires, by itself, the application of empirical equations developed for very specific (and not general) situations. The mathematical description of the injection process has been derived using a significant number of assumptions made to simplify the process. To that, one must add the changes in permeability of the filter zone and the source formation itself caused by the precipitation of various types of substances and products of corrosion processes. Because of all these factors, calculation of the pressure to overcome when injecting brine to the source rock formation can only be estimated and approximated. Having a well-prepared mathematical or numerical model, we can only describe reality with some approximation. Carrying this kind of calculation has its value and is useful if only to illuminate the scale of the problem and identify the issues that need to be overcome.

The calculations performed using the model provide confirmation of the relationships between the progressive increase in injection pressure and decrease in absorbance index observed in practice in the operation of injection wells (Figures 3 and 4). The injection pressure required also increases with the increase in the stream of liquid injected in the source layer (Figure 6) and it decreases with the increasing temperature of the liquid. Unfortunately, the decrease in injection pressure required with increased temperature results in loss of geothermal power capacity (Figure 6).

REFERENCES

- [1] Bentkowski A., Biernat H., Bujakowska K., Kapuściński J.: *Dokumentacja hydrogeologiczna zasobów eksploatacyjnych wód termalnych z utworów jury dolnej w Skierniewicach*, Arch. CAG, Warszawa – unpublished (1998).
- [2] Bodzek M., Konieczny K.: *Membrane techniques in the removal of inorganic anionic micropollutants from water environment – state of the art*, Archives of Environmental Protection, **37** (2), 15–29 (2011).
- [3] Browne P.R.L.: *Hydrothermal alteration and reservoir rock type. [in]: Lectures on geothermal geology and petrology*, UNU Geothermal Training Programme. Report 2. Reykjavik, Iceland (1984).

- [4] Bujakowski W., Kepińska B., Tomaszewska B., Banaś J., Bielec B., Pająk L., Pawlikowski M., Hołojuch G., Kasztelewicz A., Miecznik M., Balcer M.: *Wytyczne projektowe poprawy chłonności skał zbiornikowych w związku z zatłaczaniem wód termalnych w polskich zakładach geotermalnych*, Wyd. Patria, Kraków (2011).
- [5] Bujakowski W., Tomaszewska B., Kepińska B., Balcer M.: *Geothermal Water Desalination – Preliminary Studies*, Proceedings World Geothermal Congress Bali, Indonesia (2010).
- [6] Carslaw H.S., Jaeger J.C.: *Conduction of heat in solids*, Oxford at the Calderon Press (1948).
- [7] Fournier R.O.: *Application of water geochemistry to geothermal exploration and reservoir engineering*, [in:] *Geothermal systems: Principles and case histories* (ed: Rybach L., Muffler L.J.P.), John Wiley & Sons, Chichester (1981).
- [8] Giggenbach W.F.: *Chemical techniques in geothermal exploration*, [in:] *Applications of geochemistry in geothermal reservoir development (D'Amore, F. coordinator)*, UNITAR/UNDP Publication. Rome (1991).
- [9] Gunnlaugsson E.: *Aspekty chemiczne oraz metody stosowane w rozpoznawaniu i wykorzystaniu złóż geotermalnych*, [in:] *Materiały Międzynarodowych Dni Geotermalnych „Polska 2004”*, Wyd. IGSMiE PAN Kraków–Skopje (2004).
- [10] Kapuściński J., Nagy S., Długosz P., Biernat H., Bentkowski A., Zawisza L., Macuda J., Bujakowska K.: *Zasady i metodyka dokumentowania zasobów wód termalnych i energii geotermalnej oraz sposoby odprowadzania wód zużytych, poradnik metodyczny*, Ministerstwo Ochrony Zasobów Naturalnych i Leśnictwa, Warszawa (1997).
- [11] Kepińska B.: *Warunki hydrotermalne i termiczne podhalańskiego systemu geotermalnego w rejonie otworu Biały Dunajec PAN-1*, Studia. Rozprawy. Monografie, Wyd. IGSMiE PAN, Kraków No 93 (2001).
- [12] Kepińska B.: *Warunki termiczne i hydrotermalne podhalańskiego systemu geotermalnego*, Studia. Rozprawy. Monografie, Wyd. IGSMiE PAN, Kraków No 135 (2006).
- [13] McCain W.D.: *Reservoir-Fluid Property Correlations-State of the Art*, SPE Reservoir Engineering, pp 266–272 (1991).
- [14] Parkhurst D.L., Appelo C.A.J.: *User's guide to PHREEQC (version 2) – A computer program for speciation, batch-reaction, one-dimensional transport, and inverse geochemical calculations*, U.S. Geological Survey Water-Resources Investigations Report 97–4259 (1999).
- [15] Recknagel H., Sprenger E., Schramek E.R.: *Compendium wiedzy: ogrzewnictwo, klimatyzacja, ciepła woda, chłodnictwo*, OMNI SCALA, Wrocław (2008).
- [16] Tomaszewska B., Barbacki A.P.: *Wstępne rozpoznanie właściwości hydrogeochemicznych wód termalnych w rejonie Gostynina*. Technika Poszukiwań Geologicznych, Geotermia, Zrównoważony Rozwój, Wyd. IGSMiE PAN, Kraków No 1–2.
- [17] Tomaszewska B.: *Prognozowanie kolmatacji instalacji geotermalnych metodą modelowania geochemicznego, Gospodarka Surowcami Mineralnymi*, Wyd. IGSMiE PAN, Kraków, Tom 24 – Zeszyt 2/3.
- [18] Tomaszewska B.: *The use of ultrafiltration and reverse osmosis in the desalination of low mineralized geothermal waters*, Archives of Environmental Protection, **37** (3), 63–77 (2011).
- [19] Wolfram M., Raupach K.: *Methods to improve the injectivity of the Skierniewice geothermal wells, Poland*. Geothermie Neubrandenburg GmbH, Arch. PEC Geotermia Mazowiecka SA – unpublished (2010).

DYNAMIKA KOLMATACJI OTWORU CHŁONNEGO PRZY ZATŁACZANIU
WYSOKO ZMINERALIZOWANYCH WÓD TERMALNYCH W STRUKTURACH PIASKOWCOWYCH
NA NIŻU POLSKIM

Ocena dynamiki procesów związanych z powstawaniem, migracją i deponowaniem cząstek stałych w systemach geotermalnych, powodujących często kolmatację i uszkodzenia otworów i złóż, jest bardzo istotna dla identyfikacji warunków ich stabilnej i długotrwałej eksploatacji. Cząstki stałe: produkty korozji, wtórne substancje wytrącone z wody geotermalnej czy też cząstki skał zbiornikowych, mogą osadzać się w instalacji powierzchniowej oraz prowadzić do kolmatacji otworów chłonnych. W pracy zaproponowano matematyczny opis zmian w czasie indeksu chłonności oraz wymaganego ciśnienia zatłaczania wody w zamodelowanych warunkach eksploatacji dubletem otworów (otwór eksploatacyjny – chłonny) wód występujących w obrębie piaskowcowych struktur liasowych na Niżu Polskim. Dla przeprowadzenia obliczeń posłużono się rzeczywistymi danymi dotyczącymi warunków ujęcia złoża otworem Skierniewice GT-2. Podstawowym produktem

wytracania wtórnych substancji mineralnych z wody geotermalnej badanego systemu jest węglan wapnia w formie aragonitu i kalcytu. Wykazano, iż w skutek kolmatacji strefy czynnej szczególnie gwałtownie ciśnienie zatłaczania rośnie w pierwszej dobie. W kolejnych godzinach, przyrost ciśnienia ma charakter zbliżony do liniowego i sukcesywnie rośnie, osiągając wartość $\sim 2,2$ MPa po 120 godzinach. Indeks chłonności spada, szczególnie wyraźnie w okresie pierwszych 6 godzin (Fig. 4). W rozpatrywanym przedziale czasu jego wartość maleje z ponad 42 do ok. $18 \text{ m}^3/\text{h}/\text{MPa}$ po 120 godzinach od rozpoczęcia zatłaczania. Wyniki prognozy znalazły potwierdzenie w trakcie realizacji rzeczywistych badań w otworze chłonnym. Indeks chłonności w trakcie wykonywania testów hydrodynamicznych po czasie 120 godzin spadł do ok. $20 \text{ m}^3/\text{h}/\text{MPa}$.